PCCP

Accepted Manuscript

This is an *Accepted Manuscript*, which has been through the Royal Society of Chemistry peer review process and has been accepted for publication.

Accepted Manuscripts are published online shortly after acceptance, before technical editing, formatting and proof reading. Using this free service, authors can make their results available to the community, in citable form, before we publish the edited article. We will replace this *Accepted Manuscript* with the edited and formatted *Advance Article* as soon as it is available.

You can find more information about *Accepted Manuscripts* in the Information for Authors.

Please note that technical editing may introduce minor changes to the text and/or graphics, which may alter content. The journal's standard Terms & Conditions and the Ethical guidelines still apply. In no event shall the Royal Society of Chemistry be held responsible for any errors or omissions in this *Accepted Manuscript* or any consequences arising from the use of any information it contains.

ROYAL SOCIETY OF CHEMISTRY

www.rsc.org/pccp

Ultrafast Vibrational and Structural Dynamics of Dimeric Cyclopentadienyliron Dicarbonyl Examined by Infrared Spectroscopy□

Fan Yang[†*], *Pengyun Yu*[†‡], *Juan Zhao*[†], *Jipei Shi*[†‡] *and Jianping Wang*[†*]

[†]Beijing National Laboratory for Molecular Sciences; Molecular Reaction Dynamics Laboratory, Institute of Chemistry, Chinese Academy of Sciences, Beijing, 100190, P. R. China

[‡]University of Chinese Academy of Sciences, Beijing 100049, P. R. China

[*]Authors to whom correspondence should be addressed

Tel: (+86)-010-62656806; Fax: (+86)-010-62563167; E-mail: yangfan@iccas.ac.cn; jwang@iccas.ac.cn

Physical Chemistry Chemical Physics Accepted Manuscript

Abstract

In this work, we carry out steady-state, femtosecond pump-probe, and two-dimensional (2D) infrared spectroscopic studies on dimeric π-cyclopentadienyliron dicarbonyl $[CpFe(CO)_2]_2$ in the C≡O stretch vibration frequency region in CCl_4 and CH_2Cl_2. The *cis* and *trans* isomers, in terms of the position of two terminal C≡O groups, are found to coexist in the two solvents. A weak asymmetric stretching peak of the *cis*-isomer is revealed under that of the IR-active *trans*-isomer by analyzing the 2D infrared cross peak, which is supported by *ab initio* computations. Further, vibrational population relaxation is found to be both solute and solvent dependent (ranging from 21 ps to 32 ps): the fastest dynamics are found for the *trans*-isomer in polar solvent environment, which is believed to be associated with the availability and number of efficient energy accepting channels to solvent molecules. The spectral diffusion dynamics of the C≡O stretching vibrations, occurring on even fast time scale (1 ps to 3 ps), mainly exhibits solvent dependence: faster dynamics is found in polar solvent, involving weak and rapidly fluctuating hydrogen bonding interactions between CH_2 groups of solvent and the terminal carbonyls of solutes.

Keywords

2D IR spectroscopy; vibrational energy relaxation; spectral diffusion; structural dynamics; metal carbonyl stretching

Physical Chemistry Chemical Physics Accepted Manuscript

1. Introduction

Characterizing structures, structural distributions, and structural dynamics of molecules in condensed phases is of critical importance to chemistry, biology, and material sciences. For example, chemical reactions are usually multipath and multiproduct oriented, reactant and product species are involved in various stages of reactions. In equilibrium molecular systems, solvent interactions, particularly through hydrogen bond, can also cause major structural changes in solutes. Because of such constant solvent-solute interactions, equilibrium chemical exchange reactions involving dynamically structured species actually occur in any condensed-phase systems.

Transition metal carbonyl complexes are molecular systems with interesting structural and photochemical properties in condensed phases. They can participate in various important chemical events, for example, sensitizing dyes for solar energy conversions, or catalyzing chemical reactions.[1-4] $CpFe(CO)_2$ dimer ($[CpFe(CO)_2]_2$ or $Cp_2Fe_2(CO)_4$), as a typical transition metal carbonyl complex, has been investigated for many years.[5-6] It is known that $CpFe(CO)_2$ dimer can adopt multiple isomeric forms in solution.[7-9] The structures of two dominant isomers are shown in Scheme 1. Interconversions between different isomers may occur on the microsecond or slower time scale.[8,10]

Conventional infrared spectroscopy (such as FTIR or linear IR) is known as one of the condensed-phase structural sensitive spectroscopic methods. This is because each chemical group has at least one IR-active vibrational mode that can be used to characterize its local structure through vibrational frequency and intensity. However, the linear IR method is not effective in revealing structural dynamics informations. On the other hand, femtosecond

Physical Chemistry Chemical Physics Accepted Manuscript

pump-probe infrared spectroscopy has been known to be an important tool to monitor vibrational energy relaxation (VER) pathways in a molecular system. VER plays a very important role in chemical dynamics, chemical reactions, and energy transfer in solutions and other condensed phases.[11-15] Vibrational energy can flow from the excited vibrational state of a solute molecule to other vibrational states within the molecule via intramolecular vibrational relaxation or redistribution (IVR), or to surrounding solvent molecules through external (or intermolecular) vibrational relaxation (EVR).[13,16-19] The vibrational energy flow involving solvent molecules can be very different from that in gas phase, because solvent can take part in vibrational energy transfer directly or indirectly.[18-27]

The photochemistry of the $CpFe(CO)_2$ dimer under ultraviolet irradiation has been investigated by using time-resolved IR method.[28-31] In particular, the two terminal C≡O groups of the $CpFe(CO)_2$ dimer exhibit absorption bands featuring in the 1900-2100 cm^{-1} region, allowing their vibrational properties to be studied without interference from water and/or CO_2 absorptions. However, as can be seen in this work, due to the presence of multiple isomers, spectral overlap still occurs and sometime causes problem in spectral assignment. Under such circumstances, two-dimensional IR (2D IR) spectroscopy possesses significant advantages because it can stretch the IR absorption peaks from conventional one frequency axis to two frequency axes.

The 2D IR spectroscopy has become a powerful tool for examining structures and structural distributions of condensed-phase molecular systems in recent years.[32-48] In particular, metal carbonyl compounds have been studied by 2D IR spectroscopy, in equilibrium structure,[49-53] in transition state of chemical reactions,[54] as well as in labeled biomolecules.[55]

Physical Chemistry Chemical Physics Accepted Manuscript

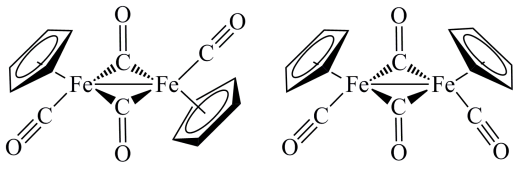

Scheme 1. Two isomers of $CpFe(CO)_2$ dimer.

In our recent works, we have studied the vibrational relaxations of $CpFe(CO)_2$ dimer using the infrared pump-probe method and found that the *cis* and *trans* isomers show similar vibrational population time, but the *trans* species orientationally diffuses slightly faster.[9] We have also studied very recently the structural dynamics of a photoproduct of $CpFe(CO)_2$ dimer under white light irradiation using the 2D IR spectroscopy, and found that the product contains two C≡O groups and exhibits vibrational quantum beat between two C≡O stretching vibrations.[56] In this work, by utilizing ultrafast IR methods and 2D IR in particular, $CpFe(CO)_2$ dimer solvated in two typical solvents, namely carbon tetrachloride (CCl_4) and dichloromethane (CH_2Cl_2), is investigated in order to further understand the ultrafast structural and vibrational dynamics of this system. The terminal (or non-bridged) C≡O stretching mode is used as vibrational probe. The vibrational transition frequency of a hidden transition of the *cis*-$CpFe(CO)_2$ dimer is determined using the 2D IR method. The population relaxation and spectral diffusion dynamics of the terminal C≡O stretching mode in the two solvents are examined and discussed in terms of solute-solvent interactions and their structural dynamics.

2. Material and Method

2.1. Sample and 1D IR Experiment

π-Cyclopentadienyliron dicarbonyl dimer (96% purity, TCI product) was used without further purification. The sample was dissolved in CCl_4 (to 18 mM concentration) or in CH_2Cl_2 (30 mM) respectively. The sample solutions were filled into a home-made liquid IR sample cell with two 2-mm thick calcium fluoride windows separated by a 50-μm thick

Physical Chemistry Chemical Physics Accepted Manuscript

Teflon spacer. IR spectra of $CpFe(CO)_2$ dimer were collected using a Nicolet 6700 FT-IR spectrometer (Thermo Electron) at a resolution of 1 cm^{-1}. To avoid sample decomposition, all IR measurements on $[CpFe(CO)_2]_2$ were carried out under dark condition at room temperature (22°C).

2.2. 2D IR Experiment

The 2D IR experimental setup has been described previously. [41-42,56] A femtosecond IR pulse with center frequency at 1980 cm^{-1} with FWHM of *ca.* 250 cm^{-1} was split into four beams by ZnSe beam splitters. Three IR pulses with wave vector k_1, k_2 and k_3 were used to produce the vibrational echo from sample, which is then amplified with the fourth IR pulse, the so-called local oscillator. Temporal delay time between the first and second pulses (k_1 and k_2) controlled by a translation stage is coherence time (τ) and that between the second and third pulses is waiting time or population time (T). Four laser pulses were set to vertical polarization for parallel 2D IR measurement. An IR monochromator equipped with a 100 line/mm IR grating and a 64 channel mercury-cadmium-telluride detector was used to collect 2D IR spectra along detection time (t) in the fashion of spectral interferometry. Post numerical Fourier transform along τ-axis yielded the frequency domain 2D IR spectra, with digital resolution of 1 cm^{-1} along both frequency axes. The projection of a 2D IR spectrum on detection frequency (ω_t), in direct comparison with an IR pump-probe signal that was collected using k_3 (pump) and an attenuated k_1 (probe) at magic-angle polarization (54.7°) condition,[41,56-58] was used to phase the 2D IR spectra. The coherence time usually scans over 2.5 ps at a step of 5 fs for a given T. A series of T-dependent 2D IR spectra were collected. The vibrational population dynamics were measured with the same magic-angle IR pump-probe experiment. Transient absorption spectra were measured from -10 ps to 100 ps at a step of 0.2 ps. Sample condition for the 2D IR measurement is the same as in 1D IR measurement described above.

Physical Chemistry Chemical Physics Accepted Manuscript

2.3. Quantum Chemistry Calculation

Geometry optimization and vibrational analysis of non-bridged C≡O stretching of *cis*-$CpFe(CO)_2$ dimer in vacuum and in different solvents using an implicit solvent model approach, namely the polarizable continuum model (PCM), were carried out at the level of the density functional theory (DFT).[59-60] Calculations were performed using B3LYP function with the 6-31++G** basis set for carbon, oxygen, hydrogen and chlorine atoms and the *sdd* pseudopotential for iron atom. Vibrational properties of CH_2Cl_2 were also analyzed at the same level. All the calculations were performed using Gaussian 09.[61] The calculation yielded eigenvalues and eigenvectors for the two C≡O stretching modes. Vibrational coupling between the two C≡O stretch modes were obtained by using a wave function de-mixing method described previously.[62-64]

3. Results and Discussion

3.1. Steady-State Linear IR Spectra

Figure 1 shows linear FTIR spectra of $CpFe(CO)_2$ dimer in CCl_4 and in CH_2Cl_2, in the frequency region of the non-bridged C≡O stretching. Mainly two peaks are shown. In CCl_4, the two peaks are located at 2004.3 and 1958.8 cm^{-1}, while in CH_2Cl_2 they are slightly red shifted (1996.9 and 1954.6 cm^{-1}). It is noted that the two absorption peaks in CH_2Cl_2 are not just simply red-shifted with respect to those in CCl_4, but are also broadened to some extent, suggesting more structural inhomogeneity in polar solvent environment (CH_2Cl_2). In addition, the ratio of the two peaks shows solvent dependence: the low-frequency component is stronger in CCl_4 but weaker in CH_2Cl_2. Previously reported linear IR spectra of $CpFe(CO)_2$ dimer dissolved in octane, carbon disulfide as well as n-hexane[7,52,65] exhibited a peak ratio similar to that in CCl_4 shown in Figure 1.

Physical Chemistry Chemical Physics Accepted Manuscript

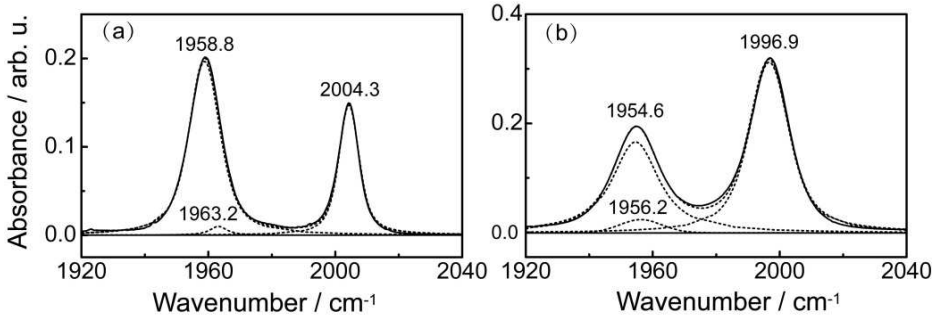

Figure 1. Linear IR spectra of non-bridged C≡O stretches of $CpFe(CO)_2$ dimer in CCl_4 (a) and in CH_2Cl_2 (b), and their fittings using Voigt function.

Table 1. Fitting parameters of the FTIR spectra of the $CpFe(CO)_2$ dimer in CCl_4 and in CH_2Cl_2 with Voigt functions.

		CCl_4		CH_2Cl_2	
species	mode assignment	peak position /cm^{-1}	peak width /cm^{-1}	peak position /cm^{-1}	peak width /cm^{-1}
cis	*ss*	2004.3	7.6	1996.9	14.9
	as [a]	1963	6.5	1956	15.6
trans	*as*	1958.8	11.7	1954.6	17.5

a. Frequency position is determined by 2D IR. See text.

Linear IR spectra can be used to deduce molecular structural information under equilibrium conditions. Here, because there are two non-bridged C≡O groups presented in this compound, the two peaks shown in Figure 1 must be due to the linear combination of the two carbonyl stretching modes, regardless of the presence of multiple isomers. To assign the IR absorption bands in this region, we first fit them with Voigt functions. Fitting parameters are listed in Table 1. Previous studies of $CpFe(CO)_2$ dimer in various solvents[9,52] have suggested that there are two prevailing isomers presented in the solvated $CpFe(CO)_2$ dimer: the *trans*-form that has two non-bridged (or terminal) C≡O groups sitting on the opposite side of the interface consisting two iron atoms and two bridged carbon atoms (Scheme 1), and the *cis*-form that has two non-bridged C≡O groups sitting on the same side of the interface. The

Physical Chemistry Chemical Physics Accepted Manuscript

assignment of the two peaks is made with the aid of computations (see below). The low-frequency component (near 1960 cm^{-1}) is mainly due to the *trans*-form, while the high-frequency component (near 2000 cm^{-1}) belongs to the *cis*-form.[9,52]

The vibrational harmonic frequencies, intensities, transition energy difference ($\Delta\nu$), vibrational coupling constants, distance between two terminal carbonyl (C≡O) bond center point and angles between two terminal carbonyls of the *cis*-$CpFe(CO)_2$ dimer, obtained by *ab initio* calculation are listed in Table 2. Previous computations[9] suggested that the *trans*-form only has one IR-active component, i.e., the asymmetric (*as*) combination of the two non-bridged C≡O stretches (denoted as *as/trans* component). The computations shown in Table 2 suggest that the *cis*-form has two IR-active components, the symmetric stretching (*ss*) of two C≡O stretches that is strong in intensity, located at the high-frequency side, and a weak asymmetric vibration (denoted as *as/cis*) that is located at the low-frequency side. This is the case for the gas phase and for the implicit PCM solvents. However, when $CpFe(CO)_2$ dimer was solvated in different solvents, the two C≡O stretches will shift their vibrational frequencies to the low-frequency side. These two frequencies in CH_2Cl_2 are lower than those in CCl_4, which is in agreement with the IR experiments. The frequency difference ($\Delta\nu$) between the *as/cis* and *ss/cis* modes is 37.0 cm^{-1} in gas and decreases in solution. The value is slightly smaller in CH_2Cl_2 than in CCl_4 (33.5 cm^{-1} vs. 36.3 cm^{-1}), agreeing with the trend of experimentally determined values (40.7 cm^{-1} vs. 41.1 cm^{-1}, see Section 3.3). Accompanying the largest $\Delta\nu$ in the gas phase, the coupling constant between the two C≡O stretches in gas is also the largest. This is because strong inter-mode coupling causes large frequency separation. This also applies to the cases in the three solvents listed in Table 2: the larger the coupling, the larger the frequency separation. Further, one sees that $\Delta\nu$ roughly equals 2β in all cases, suggesting that the two C≡O stretching local modes are nearly degenerate and the frequency separation is dominated by inter-mode coupling. This is in perfect agreement with the

Physical Chemistry Chemical Physics Accepted Manuscript

symmetric chemical environment sensed by the two terminal C≡O groups in the *cis*-form. Further more, the bond center distances and bond angles are nearly media independent, suggesting that solvent environment does not change much the molecular geometry of the *cis*-isomer.

Further, some degree of exchange between the *cis*- and *trans*-forms of $CpFe(CO)_2$ dimer exist in solution and the FTIR results suggest that the equilibrium is in favor of the *trans*-form in nonpolar solvent, evaluated by assuming the two C≡O stretching modes have the same oscillation strength.[9] Because the *cis* structure has larger permanent dipole,[9] it is more stable than the *trans*-form in polar solvent, leading to the observed higher intensity of the *cis* absorption.

Further, the frequency position of the *as*/*cis* component is lower than that of the *ss/cis* component, which is not directly seen from the FTIR spectra (Figure 1). This component believed to be hidden under that of the *as/trans* band, which can be revealed by the 2D IR spectroscopy, as shown below. In Figure 1, the 2D-IR-determined frequency for the *ss/cis* component in each solvent case is used in spectral fitting, while the intensity is determined by spectral fitting.

Table 2. Harmonic transition frequencies (ν) and intensities (I) with transition frequency difference (Δν), inter-mode coupling constant (β), bond center point distance (r) and bond angle (θ) between two terminal carbonyls of the *cis*-$CpFe(CO)_2$ dimer in different media.

media	mode [a]	ν /cm^{-1}	I /km·mol^{-1}	Δν /cm^{-1}	β /cm^{-1}	r /Å	θ /°
gas-phase	*as/cis*	2045.1	206.1	37.0	18.5	3.493	28.3
	ss/cis	2082.1	1485.3				
CCl_4	*as/cis*	2026.1	272.7	36.3	18.2	3.501	28.3
	ss/cis	2062.4	2125.8				
CH_2Cl_2	*as/cis*	2006.7	353.8	33.5	16.7	3.516	28.3
	ss/cis	2040.2	3056.8				
n-hexane	*as/cis*	2029.6	264.0	36.5	18.3	3.511	28.6
	ss/cis	2066.1	1994.8				

[a] *as* = asymmetric stretching; *ss* = symmetric stretching.

Physical Chemistry Chemical Physics Accepted Manuscript

3.2. Dynamical 2D IR Spectra

The 2D IR spectra of $CpFe(CO)_2$ dimer in the C≡O stretching region in CCl_4 and in CH_2Cl_2 at different waiting times are shown in Figure 2. Each spectrum apparently contains two pairs of diagonal peaks, and two pairs of off-diagonal peaks, with the latter being more prominent at later times. For the diagonal signals, the positive (red) and negative (blue) peaks arise from the 0→1 vibrational transition (i.e., $n = 0 \rightarrow n = 1$ where n is vibrational quantum number), and 1→2 vibrational transition, respectively. According to the band assignment in the linear IR spectra, the low-frequency diagonal signals are mainly due to the *as/trans* component while the high-frequency diagonal signals are purely due to the *ss/cis* component. Viewing along the ω_t axis, the 1→2 transition in a diagonal signal is shifted to the low-frequency side with respect to its 0→1 transition. At early T, the 2D IR diagonal signals are elongated along diagonal (solid line) for both the 0→1 and 1→2 transitions, which is the case in both solvents. As T increases the diagonal signals become more vertically tilted, indicating a process called spectral diffusion (SD).[66] Here the spectral diffusion is the evolution of frequency of a given vibration mode as a function of T, which is caused by the structural fluctuation of both solute and solvent molecules.

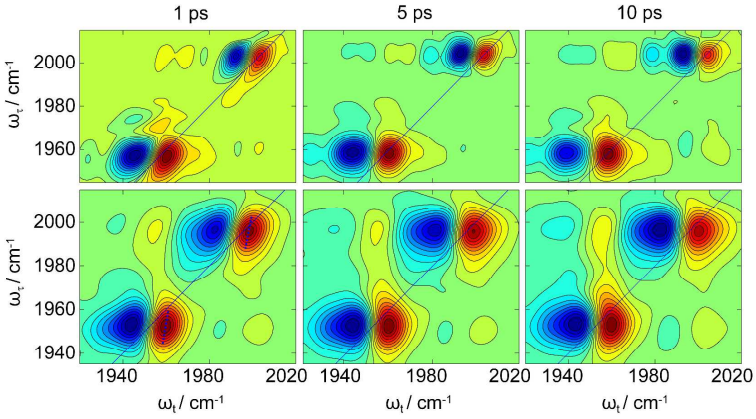

Figure 2. Waiting-time resolved absorptive 2D IR spectra in the C≡O stretching region of $CpFe(CO)_2$ dimer in CCl_4 (upper) and in CH_2Cl_2 (bottom). An example of centre line slope is shown on the diagonal 0→1 transitions in the lower left panel.

Physical Chemistry Chemical Physics Accepted Manuscript

The spectral diffusion dynamics of the C≡O stretch in $CpFe(CO)_2$ dimer in the two solvents can be characterized from the waiting-time dependent 2D IR vibrational echo spectra. Here the centre line slope (CLS) method[67-68] is used, which is the ridge line of a 2D peak with an acute angle with the $\omega_\tau = \omega_t$ direction. We extract the CLS for the 0→1 transition at different waiting times. The change of the slope can grasp the main feature of the change of shape for a 2D peak, thus it can be used to characterize the spectral diffusion dynamics. The results are given in Figure 3 with single exponential fitting. Fitting parameters are listed in Table 3.

The results show that the spectral diffusion of the C≡O stretch in $CpFe(CO)_2$ dimer occurs on the time scale of a few picoseconds. First, one sees that in the same solvent, the spectral diffusion dynamics of the high-frequency component (the *ss/cis* component) is quite similar to that of the low-frequency component, which is mainly the *as/trans* component, indicating a quite similar solute-solvent dynamical interaction for both the *cis* and *trans* isomers. In the case of CCl_4, they are almost indistinguishable within experimental error. Here because of the linewidth difference, the uncertainty in CCl_4 is larger than in CH_2Cl_2. Second, the τ_{SD} is nearly three times faster in CH_2Cl_2 than in CCl_4 (Table 3), indicating a speed up of frequency-frequency time correlation relaxations in CH_2Cl_2.

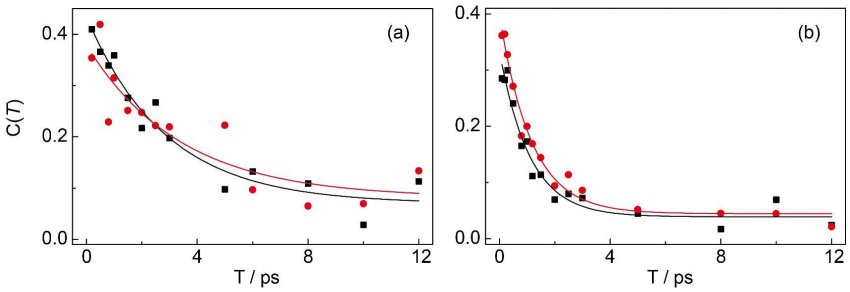

Figure 3. Centre line slopes and their fits of the C≡O stretch in $[CpFe(CO)_2]_2$ in CCl_4 (a) and CH_2Cl_2 (b). Black dots are for the *as/trans* component and the red dots are for the *ss/cis* component.

Physical Chemistry Chemical Physics Accepted Manuscript

Table 3. Fitting parameters for the centre line slope dynamics by single exponential decay for the C≡O stretches in $[CpFe(CO)_2]_2$ in CCl_4 and CH_2Cl_2.

solvent	mode	ΔC [a]	τ_{SD} /ps
CCl_4	*as/trans*	0.37	2.9±0.7
	ss/cis	0.30	3.4±0.6
CH_2Cl_2	*as/trans*	0.30	1.1±0.2
	ss/cis	0.36	1.1±0.1

a. ΔC = [C(*T*=0 ps) - C(*T*=12 ps)], indicating the amplitude of spectral diffusion.

3.3. Revealing the Hidden *as/cis* Component

2D IR spectroscopy can be used to reveal the hidden diagonal peaks in the case of coexisting peaks. First, the time-dependent 2D IR spectra in Figure 2 show cross peaks. They can be due to vibrational coupling and/or vibrational energy transfer involving the *trans*- and *cis*-isomers. We find that the cross peaks do not have ω_t equal to that of the *as/trans* mode, so that the contribution from the intermolecular vibrational interaction or energy transfer between the *trans*- and *cis*-forms can be ruled out. The *trans*-*cis* isomerization energy barrier is significant so that it occur on a much lower time scale. In fact, these 2D IR cross peaks have ω_t frequency equal to that of the *as/cis* mode (see below). This is not surprise because the *as/cis* and *ss/cis* modes are intrinsically coupled. The coupling resultant cross peaks appear to be weak but show up instantaneously (very small *T*). The evolution of the cross peaks indicates intramolecular vibrational energy redistribution between the *as/cis* and *ss/cis* modes, as has been studied using the non-rephasing 2D IR spectra in a recent work.[52] In this paper, we only focus on whether we can determine the cross peak positions reliably. This is done by plotting the projection of 2D IR spectral slices containing a known diagonal peak, and a cross peak resulting from the known diagonal peak and an unknown diagonal peak. The 2D IR spectra at several waiting times are utilized for this purpose.

Physical Chemistry Chemical Physics Accepted Manuscript

In Figure 4, we plot the slices of the absorptive 2D IR spectra (shown in Figure 2) along ω_τ = 2004 cm^{-1} in CCl_4 and ω_τ = 1997 cm^{-1} in CH_2Cl_2 at different waiting times. The projection of this cut onto the ω_t axis has four peaks, two major ones (one positive peak and one negative peak starting from the high-frequency side) and two minor ones (one positive peak and one negative peak), which can be fitted roughly by four Gaussian functions. The major positive and negative peaks located at the high-frequency side belong to the diagonal signal of the *ss/cis* component, and the minor one located at the low-frequency side belong to the cross-peak of the *as/cis* and *ss/cis* components, thus its positive peak is the peak position of the hidden *as/cis* component. During fitting the frequency and linewidth of the positive peak of the major *ss/cis* component is fixed to the values listed in Table 1. In addition, each pair of positive and negative peaks is set to roughly equal integrated area. In this way, the ω_t value of the cross peak, i.e., the ω_t of the low-frequency *as/cis* component, can be determined. Figure 4 gives the frequency position of the *as/cis* component at different waiting times in the two solvents and the mean values are summarized in Table 4. As can be seen, although the bands of the *as/cis* and *as/trans* components are overlapped in the linear IR spectra, the peak frequency of the *as/cis* component is found to be slightly higher than that of the *as/trans* component. It should be pointed out that the cross-peak positions are heavily affected by the diagonal peaks, which is particularly the case in CH_2Cl_2, where the left-top cross-peak positions in the 2D IR spectra (Figure 2, lower panels) appear to be even slightly lower than the *as/trans* peaks. Nevertheless, the frequency of the *as/cis* component is found to be 1963.2 cm^{-1} in CCl_4 and 1956.2 cm^{-1} in CH_2Cl_2, which are used in fitting the linear IR spectra in Figure 1. The frequency difference between the *as/cis* and *ss/cis* component is thus determined, which is 41.1 cm^{-1} in CCl_4 and 40.7 cm^{-1} in CH_2Cl_2 (Table 4). The photoisomerization of $CpFe(CO)_2$ dimer in cyclohexane on the microsecond time scale has been reported previously by UV flash photolysis with CO laser as probe.[69] In that work, the

Physical Chemistry Chemical Physics Accepted Manuscript

formed cis component has a low-frequency component (*as/cis*) that is also coincident with the strong peak from the reactant, the *trans* isomer (*as*/*trans*). This agrees with general understanding that the *as*/*cis* mode is coincident with the *as*/*trans*, even though the actual frequency positions cannot be directly compared with the results inCCl_4 or CH_2Cl_2 reported in our work because the solvent differs from our case.

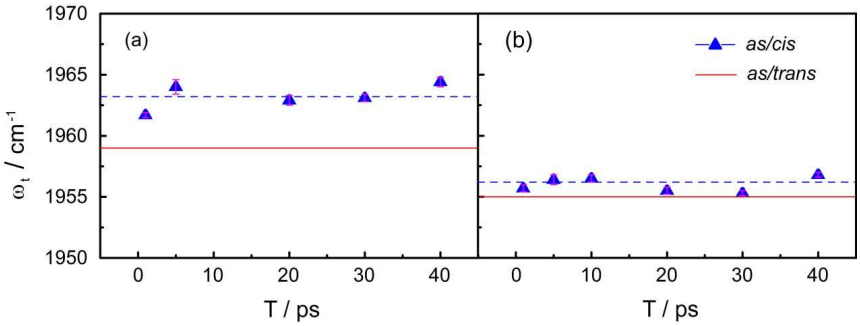

Figure 4. Terminal C≡O stretching frequency positions (triangles) and their average (dashed line) of the *as/cis* component in CCl_4 (a) and in CH_2Cl_2 (b), determined from the absorptive 2D IR spectra at different waiting times, and that of the *as/trans* component determined from the linear IR spectra shown in Figure 1 (red line).

Table 4. Mean value of frequency ($\bar{\nu}$) of the terminal C≡O stretching frequency of the *as/cis* component, frequency difference ($\Delta\nu$) between the *ss/cis* and *as/cis* components, and frequency of the *as/trans* component, of the $CpFe(CO)_2$ dimer in CCl_4 and in CH_2Cl_2.

solvent	$\bar{\nu}_{as/cis}$ /cm^{-1}	$\Delta\nu_{ss/cis\ -\ as/cis}$ /cm^{-1}	$\nu_{as/trans}$ /cm^{-1}
CCl_4	1963.2±0.4	41.1	1958.8
CH_2Cl_2	1956.2±0.3	40.7	1954.6

3.4. Vibrational Population

Using the magic-angle pump-probe method, the transient spectra in the terminal C≡O stretching region of the $CpFe(CO)_2$ dimer in CCl_4 and in CH_2Cl_2 were collected and the results were shown in Figure 5. The band assignment is the same as the case of 2D IR: there are two pairs of transient signals and the high-frequency pair is due to the *ss/cis* component,

Physical Chemistry Chemical Physics Accepted Manuscript

while the low-frequency pair is mainly due to the *as/trans* component. The blue signal corresponds to the ground-state bleaching and stimulated emission, while the red one corresponds to the excited-state absorption. In CCl_4, the transient signals appear to be generally narrower than those observed in CH_2Cl_2, which is similar to the observation in both linear IR and 2D IR results.

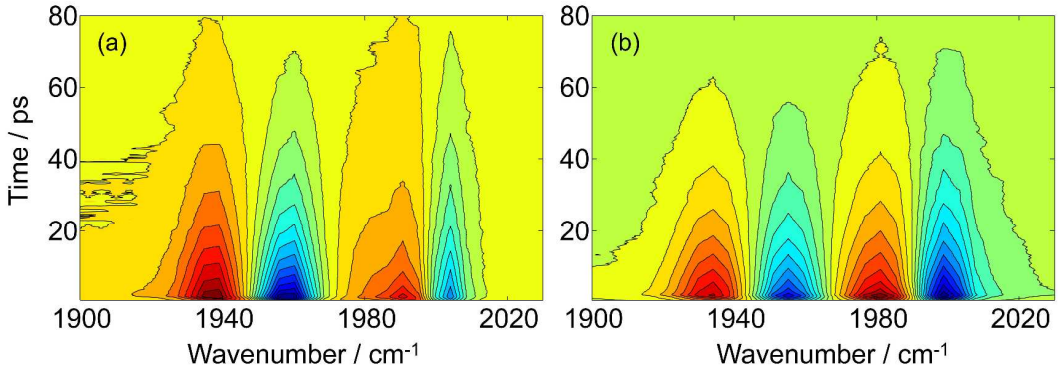

Figure 5. Magic-angle pump-probe IR spectra in the terminal C≡O stretching region of the $CpFe(CO)_2$ dimer solvated in CCl_4 (a) and in CH_2Cl_2 (b).

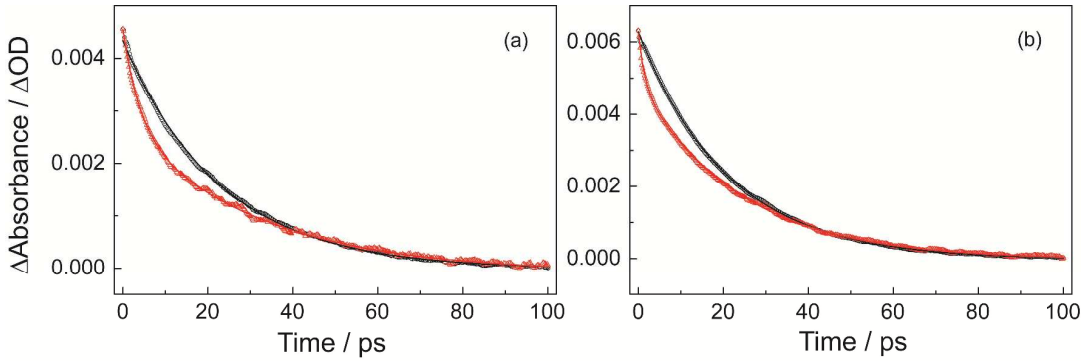

Figure 6. Vibrational population relaxation dynamics of the C≡O stretchings of $CpFe(CO)_2$ dimer solvated in CCl_4 (a) and in CH_2Cl_2 (b). Probing frequencies are: (a) 1939 cm^{-1} for the *as/trans* peak (black); 1991 cm^{-1} for the *ss/cis* peak (red); (b) 1934 cm^{-1} for the *as/trans* peak (black); 1981 cm^{-1} for the *ss/cis* peak (red). Exponential fittings are also given (solid lines).

The vibrational lifetime was extracted from the time dependent pump-probe spectra. The vibrational population relaxation of the *as/trans* component and that of the *ss/cis* component were probed at the absorption peak positions and the results are shown in Figure 6, as a

Physical Chemistry Chemical Physics Accepted Manuscript

function of the delay time between pump and probe pulses. Note that the contribution of the very small *as/cis* component is ignored for simplification. Exponential fitting yields the lifetime (T_1) of each vibrational excited state (n = 1) of the C≡O stretching modes, which are summarized in Table 5.

Table 5. Parameters fitted to single or double exponential functions of the vibrational relaxation of the C≡O stretching modes of $CpFe(CO)_2$ dimer in CCl_4 and CH_2Cl_2, in the form of $\sum_{i=a,b} A_i \exp(-T_1^i / t)$, probed at the absorption peak positions.

solvent	probe frequency /cm^{-1}	A_a /%	$T_1{}^a$ /ps	A_b /%	$T_1{}^b$/ps
CCl_4	1939 (*as/trans*)			100	22.9±0.1
	1991 (*ss/cis*)	39	3.9±0.1	61	31.8±0.4
CH_2Cl_2	1934 (*as/trans*)			100	21.5±0.1
	1981 (*ss/cis*)	22	1.5±0.1	78	23.9±0.1

The vibrational population of the *ss/cis* component in CCl_4 shows a fast relaxation time of 3.9 ps, followed by a slow relaxation time of 31.8 ps; while the two time constants in CH_2Cl_2 are both slightly shorter (1.5 ps and 23.9 ps), indicating a generally faster vibrational energy relaxation in CH_2Cl_2 than in CCl_4. The T_1 of the *as/trans* component, on the other hand, are somewhat faster than their *cis* counter part in each solvent. A previous study[52] showed similar vibrational relaxation time scales for the C≡O stretching modes in the same metal carbonyl and other similar metal carbonyl complexes. The fast component for the *cis*-isomer can be explained as rapid population equilibration between two IR-active C≡O stretching modes (i.e., the IVR process), which is absent in the *trans*-isomer because only the *as* vibration is IR active.

Further, the fast component is found to be solvent dependent, being more than twice slower in CCl_4 than in CH_2Cl_2. In a previous study[35] an anti-correlation between degree of hydrogen bonding between solute and solvent and IVR time scale of the carbonyl stretching

Physical Chemistry Chemical Physics Accepted Manuscript

mode of $Mn_2(CO)_{10}$ was observed. In that work, $Mn_2(CO)_{10}$ and a series of strong hydrogen bond donors (alcohols) interaction were studied. However, we observed a faster IVR time in a weak hydrogen bond donor solvent (CH_2Cl_2) than in the nonpolar non-hydrogen bonding solvent (CCl_4). The different observations in these two studies might be due to the strength of hydrogen bonding interactions. Further studies are needed to explore the role of solvent played in the IVR process.

3.5. Structural Dynamics and Solvent Influences

It is seen from Figure 1 that in CCl_4 the linewidth of the *as/trans* mode is somewhat broader than that of the *ss/cis* component (12.0 cm^{-1} *vs*. 8.4 cm^{-1}), while in CH_2Cl_2 both vibrations exhibit additional line-width broadening (19.0 cm^{-1} and 15.2 cm^{-1}). First, the linewidth difference between the *trans*- and *cis*-forms reflects their structural and dynamical differences. In $CpFe(CO)_2$ dimer, the two non-bridged C≡O stretches in the *trans*-form have more solvent accessibility than those in the *cis*-form, simply because in the former case nearby solvent molecules do not have to compete with each other in interacting with the two C≡O groups. In other words, in the *trans*-form terminal C≡O group can sample more solvent structures. This leads to more inhomogeneous broadening, thus a generally wider bandwidth of the *as/trans* IR component. Even though the linear IR spectrum in CH_2Cl_2 was also fitted using Voigt functions, it appears to have some features of Gaussian function (Figure 1). In addition, polar and weak protic solvent CH_2Cl_2 exerts stronger influences on the solute (through dipole-dipole interaction and weak hydrogen bonding interaction), which will contribute to frequency shifting, and linewidth broadening as well, to both the *trans* and *cis* IR components.

Further, the relatively faster population relaxation dynamics in polar solvent can be explained as solvent effect involving intermolecular energy transfer. Figure 7 shows linear IR

Physical Chemistry Chemical Physics Accepted Manuscript

spectrum of non-bridged C≡O stretches of $CpFe(CO)_2$ dimer in CH_2Cl_2, along with those of pure CH_2Cl_2 and CCl_4 in the same frequency region. Absorption bands located at 1970 and 1998 cm^{-1} can be seen in CH_2Cl_2; however, no IR-active modes can be found for CCl_4 in this region. The calculated vibrational transition frequencies and intensities of CH_2Cl_2 are summarized in Table 6. We attribute the two bands observed in CH_2Cl_2 to the combinations of CCl_2 symmetric or asymmetric stretches (ν_2 or ν_3) and CH_2 out-plane rocking (ν_6). Because these two combination bands come quite close to the two C≡O stretches of $CpFe(CO)_2$ dimer, relatively efficient vibrational energy transfer channels open up and leads to the accelerated VER rate. This is highly likely because CH_2 groups can form weak but direct hydrogen bonds with the terminal C≡O groups, for example, in the *cis*-form (Figure 8) that can facilitate vibrational energy dissipation process. Such interaction is absent in CCl_4. In addition, from CCl_4 to CH_2Cl_2, the acceleration of T_1 is more significant in the *cis*-form probably because two hydrogen bonds can be formed by the same solvent molecule so as to form a relatively rigid structure and a relatively reliable energy dissipation channel. This is perhaps also the reason of the *cis*-form to have a narrower bandwidth (Figure 7).

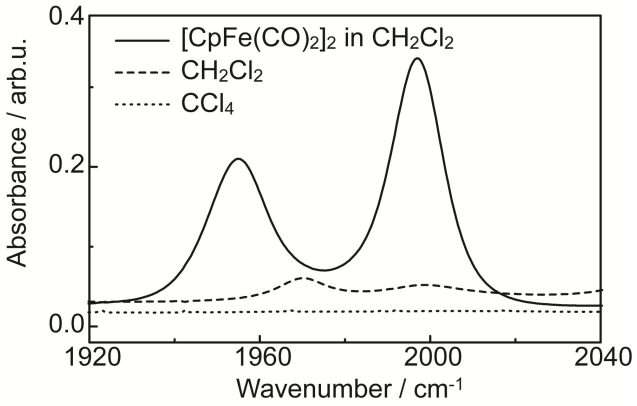

Figure 7. Linear IR spectra of $CpFe(CO)_2$ dimer in CH_2Cl_2 (solid line), pure CH_2Cl_2 (dashed line), and CCl_4 (dotted line), in the C≡O stretching frequency region.

Physical Chemistry Chemical Physics Accepted Manuscript

Table 6. Character, frequency and intensity of vibration modes in CH_2Cl_2.

mode number	mode assignment [a]	frequency /cm^{-1}	intensity / km/mol
ν_1	CCl_2 δ	281.8	0.50
ν_2	CCl_2 *ss*	700.0	13.66
ν_3	CCl_2 *as*	722.28	168.67
ν_4	CH_2 ρ	906.0	1.54
ν_5	CH_2 τ	1177.1	0.00
ν_6	CH_2 ω	1306.5	61.52
ν_7	CH_2 δ	1463.8	0.00
ν_8	CH_2 *ss*	3132.0	7.62
ν_9	CH_2 *as*	3215.7	0.00

[a] δ = scissor vibration; ρ = in-plane rocking; τ = twisting; ω = out-plane rocking.

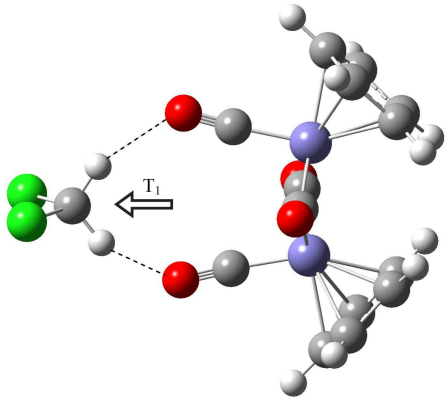

Figure 8. Hydrogen-bond aided intermolecular energy relaxations of the excited C≡O stretch of the *cis*-$CpFe(CO)_2$ dimer in CH_2Cl_2.

The spectral diffusion is found to occur within a few picoseconds for the two solvent cases, which is influenced by solute and solvent properties and solute-solvent interaction. An intuitive explanation is that, faster diffusion in polar solvent environment suggests the solvent configuration fluctuates rapidly, which may be simply associated with the fluctuating hydrogen bonds between CH_2 groups of solvent and terminal carbonyls of solutes. However, since the spectral diffusion dynamics is more related to the detailed solute-solvent interactions, there are also other possibilities, as has been discussed recently in several works

Physical Chemistry Chemical Physics Accepted Manuscript

where the spectral diffusions of a transition metal coordination compound ligands were found to depend on solvent viscosity such as $E_T(30)$, [70] Lewis acceptor number (AN),[71-72] and donor number (DN).[70] In the present case, the macroscopic viscosity values of the two solvents are different (0.908 mP·s for CCl_4 and 0.413 mP·s for CH_2Cl_2),[73] their AN and $E_T(30)$ are also quite different (AN = 8.6 and $E_T(30)$ = 32.4 kcal mol^{-1} for CCl_4; AN = 20.4 and; $E_T(30)$ = 40.7 kcal mol^{-1} for CH_2Cl_2).[74-75] It seems that the observed τ_{SD} values for the carbonyl stretching mode in $CpFe(CO)_2$ dimer, which are *ca*. 3 ps in CCl_4, and 1.1 ps in CH_2Cl_2, for both the *trans* and *cis* isomers, are positively correlated with solvent viscosity, which agrees with a recent work of $Mn_2(CO)_{10}$ in alcohols. Also, the observed τ_{SD} values are negatively correlated with both AN and $E_T(30)$. Similar negative correlation seems to be also valid if normalized E_T^N values are used (E_T^N = 0.052 for CCl_4 and E_T^N = 0.309for CH_2Cl_2). This also generally agrees with the results of sodium nitroprusside nitrosyl stretching mode reported recently,[72] but differs from the results of rhenium carbonyl compounds.[70] Even though the two cases study in the present work can not draw a linear correlation yet, the results agree with the majority of recent observations, suggesting that indeed spectral diffusions are closely related to microscopic viscous properties of solvent.

4. Conclusion

In summary, ultrafast structural and vibrational dynamics of dimeric π-cyclopentadienyliron dicarbonyl are examined using the terminal C≡O groups as probe by a combination of steady-state, transient pump-probe, and 2D IR spectroscopies. The 2D IR method is utilized to reveal the presence of the asymmetric stretching component of *cis*-$CpFe(CO)_2$ dimer that is hidden under the envelope of the IR absorption band of the *trans* isomer in both CCl_4 and CH_2Cl_2. The vibrational properties of the two vibrational mode of

Physical Chemistry Chemical Physics Accepted Manuscript

the *cis*-isomer are also examined by quantum chemistry computations utilizing implicit solvent model, and the obtained results support the experimental findings. The vibrational population of the *ss/cis* component shows a two-step fashion, in which the fast component is likely due to a rapid population equilibration between two IR-active C≡O stretching modes, which is absent in the *trans*-isomer because only its asymmetric vibration is IR active; while the slow component involves intermolecular vibrational energy dissipation through solvent combination modes, which explains the observed acceleration in the T_1 relaxation in the case of CH_2Cl_2 with respect to that case of CCl_4. The spectral diffusion of the C≡O stretching vibrations in $CpFe(CO)_2$ dimer occurs within a few picoseconds, which is the result of fast changing of solvent configuration. Faster spectral diffusion is observed in polar environment, which is probably associated with the rapid fluctuating hydrogen bonds between CH_2 groups of solvent and terminal carbonyls of solutes.

Acknowledgement

This work was supported by the Knowledge Innovation Program (Grant No. KJCX2-EW-H01). The support from the National Natural Science Foundation of China (91121020, 20727001 to JW, and 21473212 to FY) was also acknowledged.

References

1 A. J. Morris, G. J. Meyer, E. Fujita, *Acc. Chem. Res.* 2009, **42,** 1983-1993.

2 B. Zhou, H. Chen, C. Wang, *J. Am. Chem. Soc.* 2013, **135,** 1264-1267.

3 V. K. Chidara, G. Du, *Organometallics* 2013, **32,** 5034-5037.

4 R. B. Nasir Baig, R. S. Varma, *ACS Sustain. Chem. & Eng.* 2013, **1,** 805-809.

5 T. E. Bitterwolf, *Coord. Chem. Rev.* 2000, **206,** 419-450.

6 M. Jaworska, W. Macyk, Z. Stasicka, *Struct. Bond.* 2004, **106,** 153-172.

Physical Chemistry Chemical Physics Accepted Manuscript

7 F. A. Cotton, G. Yagupsky, *Inorg. Chem.* 1967, **6,** 15-20.

8 J. G. Bullitt, F. A. Cotton, T. J. Marks, *Inorg. Chem.* 1972, **11,** 671-676.

9 F. Yang, Y. Liu, J. Wang, *Acta Phys. -Chim. Sin.* 2012, **24,** 759-765.

10 J. G. Bullitt, F. A. Cotton, T. J. Marks, *J. Am. Chem. Soc.* 1970, **92,** 2155-2156.

11 D. W. Oxtoby, *Annu. Rev. Phys. Chem.* 1981, **32,** 77-101.

12 T. Elsaesser, W. Kaiser, *Annu. Rev. Phys. Chem.* 1991, **42,** 83-107.

13 J. C. Owrutsky, D. Raftery, R. M. Hochstrasser, *Annu. Rev. Phys. Chem.* 1994, **45,** 519-555.

14 A. Nitzan *Chemical Dynamics in Condensed Phases*; Oxford University Press Inc.: New York, 2006.

15 D. W. Oxtoby In *Adv. Chem. Phys.*; John Wiley & Sons, Inc., 2007.

16 A. Charvat, J. Aβmann, B. Abel, D. Schwarzer, *J. Phys. Chem. A* 2001, **105,** 5071-5080.

17 D. J. Nesbitt, R. W. Field, *J. Phys. Chem.* 1996, **100,** 12735-12756.

18 L. K. Iwaki, D. D. Dlott, *J. Phys. Chem. A* 2000, **104,** 9101-9112.

19 M. Banno, S. Sato, K. Iwata, H. Hamaguchi, *Chem. Phys. Lett.* 2005, **412,** 464-469.

20 B. J. Gertner, K. R. Wilson, J. T. Hynes, *J. Chem. Phys.* 1989, **90,** 3537-3558.

21 W. P. Keirstead, K. R. Wilson, J. T. Hynes, *J. Chem. Phys.* 1991, **95,** 5256-5267.

22 M. Berg, D. A. Vanden Bout, *Acc. Chem. Res.* 1997, **30,** 65-71.

23 T. Kiba, S.-i. Sato, S. Akimoto, T. Kasajima, I. Yamazaki, *J. Photochem. Photobio. A: Chem.* 2006, **178,** 201-207.

24 K. Iwata, H.-o. Hamaguchi, *J. Phys. Chem. A* 1997, **101,** 632-637.

25 S. A. Egorov, J. L. Skinner, *J. Chem. Phys.* 1996, **105,** 7047-7058.

26 J. A. Poulsen, G. Nyman, S. Nordholm, *J. Phys. Chem. A* 2003, **107,** 8420-8428.

27 D. V. Shalashilin, M. S. Child, *J. Chem. Phys.* 2003, **119,** 1961-1969.

28 J. N. Moore, P. A. Hansen, R. M. Hochstrasser, *J. Am. Chem. Soc.* 1989, **111,** 4563-4566.

29 S. Zhang, T. L. Brown, *J. Am. Chem. Soc.* 1993, **115,** 1779-1789.

30 M. W. George, T. P. Dougherty, E. J. Heilweil, *J. Phys. Chem.* 1996, **100,** 201-206.

31 P. A. Anfinrud, C. H. Han, T. Lian, R. M. Hochstrasser, *J. Phys. Chem.* 1991, **95,** 574-578.

32 R. M. Hochstrasser, *Proc. Natl. Acad. Sci. U. S. A.* 2007, **104,** 14190-14196.

33 K. Ramasesha, L. De Marco, A. Mandal, A. Tokmakoff, *Nat. Chem.* 2013, **5,** 935-940.

34 A. D. Hill, M. C. Zoerb, S. C. Nguyen, J. P. Lomont, M. A. Bowring, C. B. Harris, *J. Phys. Chem. B* 2013, **117,** 15346-15355.

Physical Chemistry Chemical Physics Accepted Manuscript

35 J. T. King, J. M. Anna, K. J. Kubarych, *Phys. Chem. Chem. Phys.* 2011, **13,** 5579-5583.

36 C. Kolano, J. Helbing, M. Kozinski, W. Sander, P. Hamm, *Nature* 2006, **444,** 469-472.

37 M. Cho, *Chem. Rev.* 2008, **108,** 1331-1418.

38 S. D. Moran, A. M. Woys, L. E. Buchanan, E. Bixby, S. M. Decatur, M. T. Zanni, *Proc. Natl. Acad. Sci. U. S. A.* 2012, **109,** 3329-3334.

39 H. Maekawa, M. De Poli, C. Toniolo, N.-H. Ge, *J. Am. Chem. Soc.* 2009, **131,** 2042-2043.

40 H. Bian, X. Wen, J. Li, H. Chen, S. Han, X. Sun, J. Song, W. Zhuang, J. Zheng, *Proc. Natl. Acad. Sci. U.S.A.* 2011, **108,** 4737-4742.

41 P. Yu, F. Yang, J. Zhao, J. Wang, *J. Phys. Chem. B* 2014, **118,** 3104-3114.

42 D. Li, F. Yang, C. Han, J. Zhao, J. Wang, *J. Phys. Chem. Lett.* 2012, **3,** 3665-3670.

43 F. Yang, P. Yu, J. Zhao, J. Wang, *ChemPhysChem.* 2013, **14,** 2497-2504.

44 J. Wang, *J. Phys. Chem. B* 2007, **111,** 9193-9196.

45 P. Hamm, J. Helbing, J. Bredenbeck, *Annu. Rev. Phys. Chem.* 2008, **59,** 291-317.

46 J. P. Ogilvie, K. J. Kubarych, *Adv. At., Mol., Opt. Phys.* 2009, **57,** 249-321.

47 N. T. Hunt, *Dalton Trans.* 2014, **43,** 17578-17589.

48 *Ultrafast Infrared Vibrational Spectroscopy*; M. D. Fayer, Ed.; CRC Press, 2013.

49 M. Khalil, N. Demirdöven, A. Tokmakoff, *J. Phys. Chem. A* 2003, **107,** 5258-5279.

50 O. Golonzka, M. Khalil, N. Demirdöven, A. Tokmakoff, *J. Chem. Phys.* 2001, **115,** 10814-10828.

51 R. Kania, A. I. Stewart, I. P. Clark, G. M. Greetham, A. W. Parker, M. Towrie, N. T. Hunt, *Phys. Chem. Chem. Phys.* 2010, **12,** 1051-1063.

52 J. M. Anna, J. T. King, K. J. Kubarych, *Inorg. Chem.* 2011, **50,** 9273-9283.

53 D. E. Rosenfeld, Z. Gengeliczki, B. J. Smith, T. D. P. Stack, M. D. Fayer, *Science* 2011, **334,** 634-639.

54 J. F. Cahoon, K. R. Sawyer, J. P. Schlegel, C. B. Harris, *Science* 2008, **319,** 1820-1823.

55 J. T. King, M. R. Ross, K. J. Kubarych, *J. Phys. Chem. B* 2012, **116,** 3754-3759.

56 F. Yang, P. Yu, J. Shi, J. Zhao, X. He, J. Wang, *Chin. J. Chem. Phys.* 2013, **26,** 711-718.

57 Y. Liu, F. Yang, J. Wang, *Acta Chimica Sinica* 2013, **71,** 761-768.

58 C. Han, J. Zhao, F. Yang, J. Wang, *J. Phys. Chem. A* 2013, **117,** 6105-6115.

59 E. Cancès, B. Mennucci, J. Tomasi, *J. Chem. Phys.* 1997, **107,** 3032-3041.

60 B. Mennucci, J. Tomasi, *J. Chem. Phys.* 1997, **106,** 5151-5158.

61 *Gaussian 09, Revision A.02,*; M. J. Frisch, G. W. Trucks, H. B. Schlegel, G. E. Scuseria, M. A. Robb, J. R.

Physical Chemistry Chemical Physics Accepted Manuscript

Cheeseman, G. Scalmani, V. Barone, B. Mennucci, G. A. Petersson, H. Nakatsuji, M. Caricato, X. Li, H. P. Hratchian, A. F. Izmaylov, J. Bloino, G. Zheng, J. L. Sonnenberg, M. Hada, M. Ehara, K. Toyota, R. Fukuda, J. Hasegawa, M. Ishida, T. Nakajima, Y. Honda, O. Kitao, H. Nakai, T. Vreven, J. A. Montgomery, Jr., J. E. Peralta, F. Ogliaro, M. Bearpark, J. J. Heyd, E. Brothers, K. N. Kudin, V. N. Staroverov, R. Kobayashi, J. Normand, K. Raghavachari, A. Rendell, J. C. Burant, S. S. Iyengar, J. Tomasi, M. Cossi, N. Rega, J. M. Millam, M. Klene, J. E. Knox, J. B. Cross, V. Bakken, C. Adamo, J. Jaramillo, R. Gomperts, R. E. Stratmann, O. Yazyev, A. J. Austin, R. Cammi, C. Pomelli, J. W. Ochterski, R. L. Martin, K. Morokuma, V. G. Zakrzewski, G. A. Voth, P. Salvador, J. J. Dannenberg, S. Dapprich, A. D. Daniels, O. Farkas, J. B. Foresman, J. V. Ortiz, J. Cioslowski, D. J. Fox, Eds.: Gaussian, Inc., Pittsburgh PA, 2009.

62 J. Wang, R. M. Hochstrasser, *Chem. Phys.* 2004, **297,** 195-219.

63 J. Zhao, J. Wang, *J. Phys. Chem. B* 2010, **114,** 16011-16019.

64 J. Zhao, J. Shi, J. Wang, *J. Phys. Chem. B* 2014, **118,** 94-106.

65 P. McArdle, A. R. Manning, *J. Chem. Soc. A: Inorg. Phys. Theo.* 1970**,** 2128-2132.

66 A. Ghosh, R. M. Hochstrasser, *Chem. Phys.* 2011, **390,** 1-13.

67 K. Kwak, S. Park, I. J. Finkelstein, M. D. Fayer, *J. Chem. Phys.* 2007, **127,** 124503-124517.

68 K. Kwak, D. E. Rosenfeld, M. D. Fayer, *J. Chem. Phys.* 2008, **128,** 204505-204510.

69 B. D. Moore, M. Poliakoff, J. J. Turner, *J. Am. Chem. Soc.* 1986, **108,** 1819-1822.

70 L. M. Kiefer, K. J. Kubarych, *J. Phys. Chem. A* 2015, **119,** 959-965.

71 B. H. Jones, C. J. Huber, A. M. Massari, *J. Phys. Chem. C* 2011, **115,** 24813-24822.

72 J. F. Brookes, K. M. Slenkamp, M. S. Lynch, M. Khalil, *J. Phys. Chem. A* 2013, **117,** 6234-6243.

73 W. M. Haynes *CRC Handbook of Chemistry and Physics on DVD, Version 2012*; CRC Press, 2011.

74 C. Reichardt, *Chem. Rev.* 1994, **94,** 2319-2358.

75 C. Reichardt *Solvents and Solvent Effects in Organic Chemistry. 2nd Ed*; VCH Verlagsgesellschaft, 1988.

Physical Chemistry Chemical Physics Accepted Manuscript

Ultrafast Vibrational and Structural Dynamics of Dimeric Cyclopentadienyliron Dicarbonyl Examined by Infrared Spectroscopy

Fan Yang[*]*, Pengyun Yu, Zhao Juan, Jipei Shi and Jianping Wang*[*]

Highlight:

Equilibrium and ultrafast structural dynamics of a classic transition metal carbonyl compound were revealed by linear and nonlinear infrared methods.

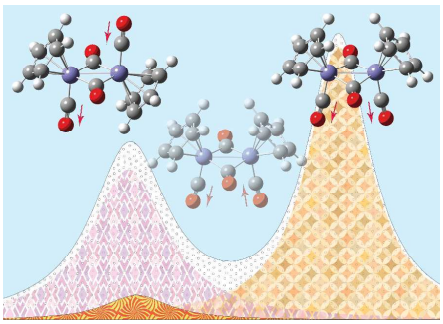

Physical Chemistry Chemical Physics Accepted Manuscript